DOI:10.22337/2587-9618-2024-20-2-163-176

OVERALL ASSESSMENT OF DEFORMATION AND FORCE OF DIAPHRAGM WALL JOINTS DURING THE STAGES OF DEEP EXCAVATION CONSTRUCTION

Phuong Tuan Nguyen [1], Truong Xuan Dang [2], Thuan Anh Nguyen [3], Hoa Van Vu Tran [3]

[1] Mien Tay Construction University, Vinh Long Province, VIETNAM
[2] Ho Chi Minh University of Natural Resources and Environment, Ho Chi Minh City, VIETNAM
[3] University of Transport Ho Chi Minh City, Ho Chi Minh City, VIETNAM

Abstract: In the realm of geotechnical engineering, deep excavation projects face intricate challenges, especially concerning the stability of barrette walls, which are highly susceptible to deformation and stress at their joints. This study focuses on evaluating the deformation and force behavior of barrette wall joints at the position of greatest deformation. The Finite Element Method (FEM) is utilized to simulate the behavior of these structures under various load conditions. The Analysis of Variance (ANOVA) method is employed to statistically analyze the FEM data, assessing the impact of different factors on deformation and force distributions within the barrette wall joints. The specific objective of this study is to determine the statistical significance of the observed deformations and understand the influence of construction stages on joint integrity. This methodological synergy enhances the predictability of engineering assessments and ensures that design and construction decisions are grounded in solid empirical evidence. The study's findings emphasize the importance of precise monitoring and advanced predictive techniques to mitigate potential risks associated with deep excavations, particularly at critical joint locations. The results indicate that the deformation patterns are primarily influenced by the geometrical setup of the walls and the mechanical properties of the soils. The greatest deformations were typically observed where the wall joints experienced the highest bending moments and shear forces, conditions exacerbated by unfavorable soil mechanics and hydrostatic pressures. The clear and consistent increase in total displacement highlights the progressive destabilization of the wall as the excavation depth increases. By integrating ANOVA with FEM, this study contributes to enhancing safety and efficiency in deep excavation projects by ensuring that decisions are grounded in empirical evidence.

Keywords: Barrette walls, Deep excavation, Finite element method, Wall thickness optimization, ANOVA tests, Deformation, Construction strategies

ОБОБЩЕННАЯ ОЦЕНКА ДЕФОРМАЦИЙ И УСИЛИЙ В СОЕДИНЕНИЯХ МЕМБРАННЫХ СТЕН НА ЭТАПАХ ВОЗВЕДЕНИЯ ОБЪЕКТОВ ГЛУБОКОГО ЗАЛОЖЕНИЯ

Фыонг Туан Нгуен [1], Чыонг Суан Данг [2], Туан Ань Нгуен [3], Хоа Ван Ву Чан [3]

[1] Миентай строительный университет, г. Виньлонг, ВЬЕТНАМ
[2] Хошиминский университет природных ресурсов и окружающей среды, г. Хошимин, ВЬЕТНАМ
[3] Хошиминский университет транспорта, г. Хошимин, ВЬЕТНАМ

Аннотация: В сфере геотехнической инженерии, при проектировании объектов глубоких заложения сталкиваются со сложными проблемами, особенно касающихся устойчивости барретных стенок, которые очень чувствительны к деформациям и напряжениям в местах их стыков. Данное исследование направлено на оценку деформации и силового поведения соединений стеновых заколок в состоянии наибольших деформаций. Метод конечных элементов (МКЭ) используется для моделирования поведения этих конструкций при различных условиях нагрузки. Метод дисперсионного анализа (ANOVA) используется для статистического анализа данных полученных МКЭ, оценки влияния различных факторов на деформацию и распределение усилий внутри заколочных соединений стенок.

Конкретная цель данного исследования – определить статистическую значимость наблюдаемых деформаций и понять влияние этапов строительства на целостность соединений. Такая методологическая синергия повышает предсказуемость инженерных оценок и гарантирует, что решения по проектированию и строительству основываются на надежных эмпирических данных. Результаты исследования подчеркивают важность точного мониторинга и передовых методов прогнозирования для снижения потенциальных рисков, связанных с эксплуатацией объектов глубокого заложения, особенно в критических местах соединений. Результаты показывают, что на характер деформаций в первую очередь влияют геометрическое расположение стен и механические свойства грунтов. Наибольшие деформации обычно наблюдались там, где стыки стен испытывали самые высокие изгибающие моменты и усилия сдвига, причем это состояние усугублялось неблагоприятной механикой грунта и гидростатическим давлением. Явное и последовательное увеличение общего смещения подчеркивает прогрессирующую дестабилизацию стены по мере увеличения глубины положения объекта. Интегрирация ANOVA с МКЭ в этом исследовании способствует повышению безопасности и эффективности проектов объектов глубоких заложения, гарантируя, что решения основаны на эмпирических данных.

Ключевые слова: Стены-барреты, глубокое заложение, метод конечных элементов, оптимизация толщины стен, тесты ANOVA, деформация, стратегии строительства

1. INTRODUCTION

In the realm of geotechnical engineering, the structural stability of deep excavation projects presents a complex interplay of challenges that demand rigorous analysis and precise monitoring [1]. As urban centers grow and the demand for underground space increases, so too does the complexity of ensuring the safety and integrity of deep foundations such as barrette walls [2, 3]. These structures, crucial for supporting large loads in poor soil conditions, are particularly susceptible to deformation and stress at their joints, which can compromise the overall stability of the construction project. The evaluation of deformation and forces at the most critical points of these structures is not just a technical necessity but a safety imperative. This study focuses on providing a comprehensive evaluation of the deformation and force behavior of barrette wall joints at the point of greatest deformation, utilizing the Finite Element Method (FEM) to simulate the intricate behaviors of these structures under various load conditions. The FEM is renowned for its ability to provide detailed insights into the stress-strain relationships and deformation characteristics of complex structures [4, 5], making it an indispensable tool in modern geotechnical engineering.

However, the vast amount of data generated by FEM simulations poses a significant challenge in terms of analysis and interpretation. This is where the Analysis of Variance (ANOVA) method comes into play [6, 7]. ANOVA is employed in this research to statistically analyze the FEM data, allowing us to systematically assess the impact of different factors on the deformation and force distributions within the barrette wall joints [8]. This statistical approach not only enhances the reliability of the simulation results but also helps in identifying key patterns and anomalies that could inform better construction practices and risk management strategies. The criticality of this approach stems from recent failures observed in similar engineering projects, where unforeseen deformations led to catastrophic failures, causing not only financial losses but also endangering human lives. Such incidents underscore the urgent need for advanced predictive and analytical techniques that can provide a more accurate and comprehensive understanding of potential risks associated with deep excavations.

By integrating ANOVA with FEM, this study aims to evaluate the overall deformation and force of the diaphragm wall joint at the weakest position [9, 10]. The specific objectives are to determine the statistical significance of the observed deformations and understand the influence of different construction stages on joint integrity. This methodological synergy enhances the predictability of engineering assessments and ensures that design and construction decisions are grounded in solid empirical evidence.

2. METHODS

2.1. Materials

The geological setup of the excavation site comprises two primary layers: the upper layer consists of mixed clay extending 7.5 meters deep, followed by a sandy soil layer with a thickness of 32.5 meters. At this site, an excavation pit measuring 11 meters by 44 meters is situated adjacent to a single-story building, with a targeted depth of 15 meters. Excavation activities are initiated from both ends of the site to optimize access and efficiency [11, 12].

To ensure the stability of the excavation walls and prevent any structural failures, a comprehensive shoring system consisting of four layers is strategically employed. These layers are positioned at various depths: -1 meter, -4.6 meters, -7.1 meters, and -9.6 meters. The structure of the shoring system is reinforced with H-beam steel sections, each measuring 400x400 mm, which are critical in maintaining the structural integrity of the excavation walls (Table 1).

Table 1. Parameters describing shoring system materials

Parameter	Value
Material type	Elastic
Y (kN/m3)	78.5
A (m2)	0.02187
I2 (m4)	0.666E-3
I3 (m4)	0.224E-3
E (kN/m2)	210.0E6

Above these walls, a cap beam with dimensions of 800x800 mm is installed to connect the barrette walls, further enhancing the stability of the overall structure. The barrette walls themselves are 800 mm thick and extend down to a length of 25 meters (Table 2). The presence of groundwater at a depth of -4 meters adds an additional layer of complexity to the excavation process [13].

The methodology employed for excavating this site starts with the installation of the cap beam, which is crucial for providing lateral support and stability from the outset. This initial step forms the foundation for all subsequent excavation and shoring activities. After the cap beam is securely in place, excavation begins with the careful removal of the soil layer (Table 3). Following this, the first layer of the shoring system is constructed. This system is vital as it offers temporary support to the excavation walls, effectively preventing their collapse.

As the excavation progresses deeper, careful management of the groundwater table is necessary [14-16]. The water table is gradually lowered to counteract hydrostatic pressure, thus mitigating the risk of water inflow that could destabilize the excavation site. This iterative process of excavation, shoring installation, and water table management is repeated meticulously with each descending layer of soil, ensuring that the excavation progresses in a controlled and safe manner toward the desired depth (Figure 1).

Table 2. Cap beam material description parameters

Parameter	Value
Material type	Elastic
Y (kN/m3)	25
Height (m)	0.8
Width (m)	0.8
A (m2)	0.02187
I2 (m4)	0.666E-3
I3 (m4)	0.224E-3
E (kN/m2)	210.0E6

Table 3. Altitude of excavated soil layers

No	The soil layer	Altitude (m)
1	Layer 1	0 – (-2)
2	Layer 2	(-2) – (-5.1)
3	Layer 3	(-5.1) – (-7.6)
4	Layer 4	(-7.6) – (-10.1)
5	Layer 5	(-10.1)–(-13.1)
6	Layer 6	(-13.1) – (-15)

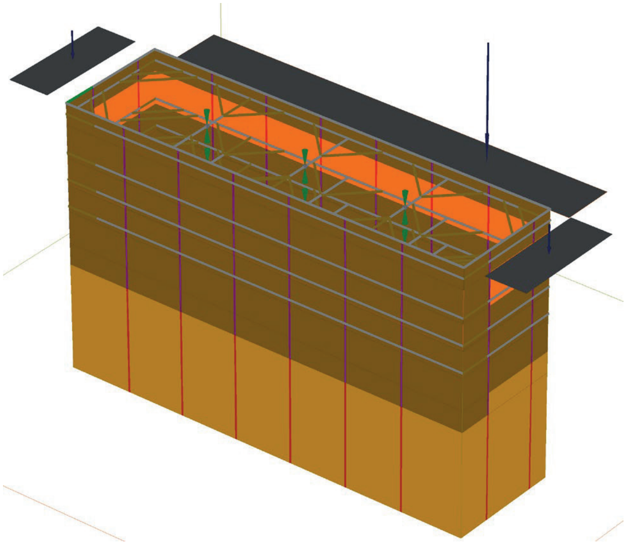

Figure 1. Overview of excavation pit models

2.2. Methods

This research meticulously investigates the deformation of barrette wall joints in deep excavation sites, employing the Finite Element Method (FEM) to conduct a detailed analysis of the soil-structure interactions under various loading and environmental conditions [17, 18]. The complex dynamics inherent in such constructions require a nuanced understanding of how different stressors—such as soil pressure, moisture variations, and adjacent structural activities—affect the structural integrity and behavior of excavation walls.

In the methodological framework of this study, a generic FEM model is constructed to represent both the geometry and material properties of the barrette walls and the surrounding soil (Table 4) [19].

This model effectively incorporates key parameters, including the elasticity, permeability, and plasticity of the soil, as well as the mechanical properties of the concrete used in the barrette walls and diaphragm wall joints has a length of 200 mm (Table 5).

By simulating the excavation process, a comprehensive analysis of how deformations collectively affect the barrette wall joint and the overall structural integrity of the walls is enabled.

In this study, we employed the Analysis of Variance (ANOVA) to examine whether there are statistically significant differences in technical parameters across various excavation stages (Figure 2) [20]. Data were collected for axial forces, bending moments, shear forces, and torsion moments from six distinct stages of excavation. Each parameter was measured at specific nodes and elements, providing a comprehensive dataset suitable for multivariate analysis. The primary goal was to evaluate the impact of changes in excavation techniques and geotechnical conditions on structural integrity and to identify any patterns or anomalies.

Table 4. Soil description parameters with Hardening soil model

Parameter	Soil type	
	Clay	**Sand**
Soil model	Hardening soil	Hardening soil
Drainage	Undrained	Undrained
γ_w (kN/m^2)	20.25	20.12
γ_{sat}	20.57	20.55
e_{init}	0.5879	0.5810
n_{init}	0.3702	0.3675
E_{50}^{ref}	6875	13.45E3
$E_{ode}^{\ ref}$	6875	13.45E3
$E_{ur}^{\ ref}$	20.63E3	40.35E3
V_{ur}	0.2	0.2
Power (m)	0.8	0.65
P^{ref}	38	400
C' ref	7.1	5.7
φ' (°)	30.40	30
Ψ (°)	0.4	0
K_z (m/day)	1.43E-05	6.91E-6
$K_x = K_y$	3.59E-05	0.138E-3

Table 5. Description parameters of barrette wall and diaphragm wall joints material

Parameter	Barrette Walls	Diaphragm Wall Joints
Material type	Elastic	Elastic
Y (kN/m3)	8	8
E1 (kN/m2)	32.50E6	32.50E6
E2 (kN/m2)	32.50E6	32.50E6
D (m)	0.8	0.8
G12 (kN/m2)	16.25E6	0.0001
G13 (kN/m2)	16.25E6	13.54E6
G23 (kN/m2)	16.25E6	0.0001

2.3. ANOVA Analysis

ANOVA was conducted by first ensuring that the data met the assumptions of normality and homogeneity of variances, which were assessed using Levene's test, respectively [21]. After confirming the assumptions, one-way ANOVA was applied to compare the mean values of each technical parameter between different stages [22, 23]. Post-hoc comparisons were performed using the Games-Howell test to determine which stages differed significantly from each other [24, 25]. This statistical approach provided a robust framework for interpreting the complexities of geotechnical behavior during progressive excavation stages [26].

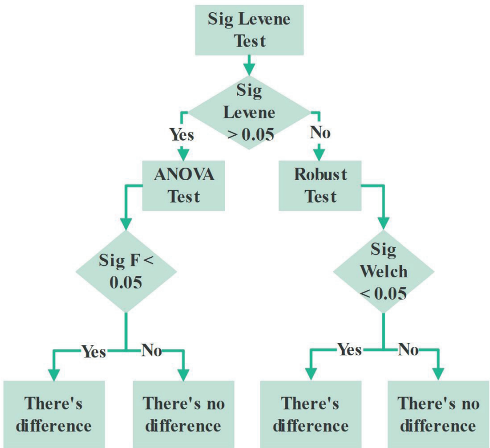

Figure 2. ANOVA General Inspection Process

3. RESULTS AND DISCUSSION

3.1. Analyze model deformation and forces

The research, through the application of the Finite Element Method (FEM), reveals that the deformation of barrette walls is significantly influenced by a combination of soil characteristics, wall geometry, and external loading conditions (Figure 3).

Total displacements |U| The largest is 0.0555 m at the red spot in Figure 3. This is the deformation analyzed at the time when it was dug to a height of -15 m.

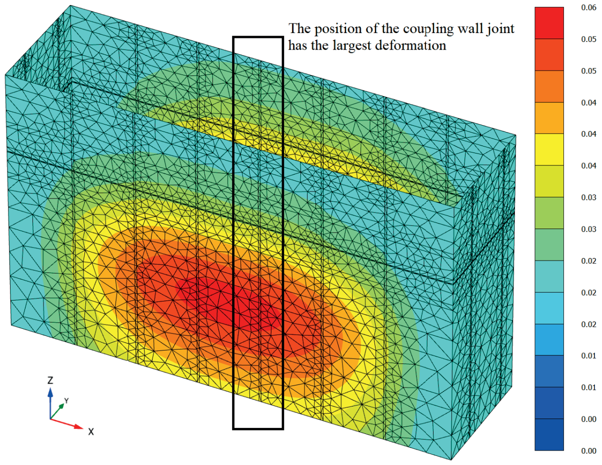

Figure 3. Deformation |U| of the barrette wall and the location of the largest deformed diaphragm wall joints

The research conducts an analysis of the deformation, shear force, and moment parameters at this diaphragm wall joint site.

From the initial to the final stage of excavation, there is a clear and consistent increase in the total displacement (|U|), which suggests a progressive destabilization of the wall as the excavation depth increases (Table 6). Starting from a minimal displacement of 0.0063 meters in the first stage, the displacement escalates to 0.0532 meters by the sixth stage. This pattern of increasing displacement is a typical response in excavation projects, reflecting the cumulative effect of stress and strain on the structure as more soil layers are removed. Deformation |U| through the stages of earthdigging are depicted in Figure 4.

Table 6. Deformation statistics of diaphragm wall joints during earthworks

Stages	Total displacements |U|	Total displacements Ux min	Total displacements Ux max	Total displacements Uy min	Total displacements Uy max	Total displacements Uz min	Total displacements Uz max
1	6.30E-03	-1.22E-05	1.21E-05	1.66E-03	4.55E-03	4.30E-03	4.37E-03
2	0.01707	-3.7E-05	3.97E-05	0.003566	0.0128	0.0112	0.0113
3	2.64E-02	-6.16E-05	5.78E-05	2.44E-03	2.10E-02	1.59E-02	1.61E-02
4	3.46E-02	-9.41E-05	7.23E-05	1.47E-03	2.83E-02	1.98E-02	2.00E-02
5	4.41E-02	-1.41E-04	8.38E-05	6.80E-04	3.78E-02	2.25E-02	2.28E-02
6	5.32E-02	-1.73E-04	8.78E-05	1.53E-04	4.80E-02	2.27E-02	2.30E-02

Displacements in the Ux axis (lateral) show a fluctuation within a narrow range, but there's a noticeable trend where the maximum displacement slightly increases from 0.0000121 meters in the first stage to 0.0000878 meters in the last stage. This indicates lateral movements are relatively controlled but do increase as the excavation progresses. Uy and Uz displacements (vertical and longitudinal), however, exhibit more substantial changes. The vertical displacement (Uz) increases significantly from 0.0043 meters in the first stage to 0.023 meters in the sixth stage, highlighting a notable vertical settling or sinking of the wall under the excavation load.

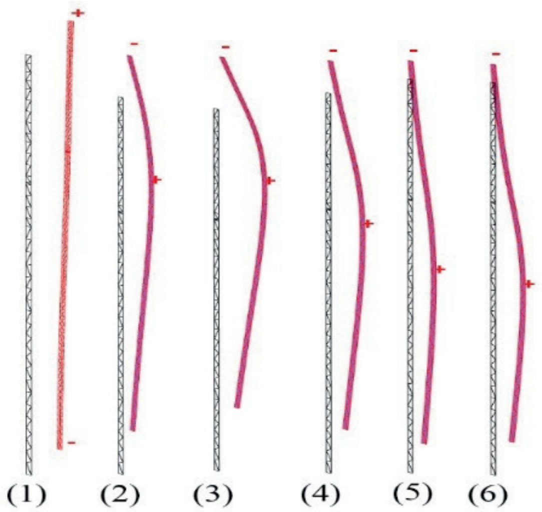

Figure 4. Deformation change |U| through the stages

The observed displacement patterns across Ux, Uy, and Uz axes suggest that while lateral stability is maintained to a certain extent, the primary challenge lies in managing vertical and longitudinal stresses. The consistent increase in these displacements indicates that the wall experiences significant downward and outward forces, which could be attributed to the unloading of soil and the consequent redistribution of stresses within the soil mass and the wall structure.

Throughout these stages of earthwork, there is a noticeable trend of increasing absolute values in both minimum and maximum axial forces for N1 and N2 (Table 7). This suggests a progressive escalation in structural loads as the excavation deepens, which is typical in such operations due to the increasing depth and the subsequent impact on lateral earth pressures.

Table 7. Axial forces value statistics

Stages	Axial forces N1		Axial forces N2	
	min	max	min	max
1	-81.04	55.05	-327	248.1
2	-257	264.5	-553.5	447.2
3	-418.6	416.4	-611.2	507.1
4	-662.8	536.6	-620.7	522.2
5	-1050	627.3	-612	519.1
6	-1329	653.7	-839.3	502.8

In the initial stage, axial forces are relatively low, indicating lesser stress and strain on the structure. As the excavation progresses to stages 2 through 6, there is a significant increase in both the compressive and tensile forces. This increment points towards growing challenges in maintaining structural stability, demanding enhanced reinforcement or support systems in deeper excavation stages.

For axial force N1, the shift from predominantly negative values in the early stages to a mixed range in the later stages highlights varying stress conditions, possibly due to changes in earth pressure or the activation of support systems like anchors or struts. Similarly, axial force N2 shows a broadening range between the minimum and maximum values, reflecting the uneven distribution of loads across the structure, which could be attributed to asymmetrical excavation or irregular soil conditions.

Notably, as the stages progress, both M11 and M22 show substantial increases in their maximum values, indicating heightened structural stresses due to deeper excavation (Table 8).

For M11, the minimum value starts at -14.07 kN/m in the first stage and drops slightly to -29.4 kN/m by the sixth stage, showing a moderate downward trend. On the other hand, the maximum value significantly increases from 20.5 kN/m in the first stage to 229.5 kN/m in the sixth stage. This sharp rise suggests that elements experiencing M11 forces are increasingly subjected to tensile stress as the excavation deepens.

M22 illustrates a more pronounced trend with even larger fluctuations. Starting from a minimum of -28.51 kN/m in stage one and plummeting to -716.5 kN/m in stage six, coupled with a maximum of 10.53 kN/m in the first stage surging to 1306 kN/m in the last stage. These values are indicative of the critical bending loads that the structure must withstand as lateral earth pressures intensify with each subsequent stage of excavation.

Table 8. Moment value statistics through mining stages

Stages	Bending M11		Bending M22	
	min	max	min	max
1	-14.07	20.5	-28.51	10.53
2	-12.4	43.08	-53.6	289.2
3	-7.627	87.1	-124.4	527.9
4	-10.2	116.7	-251.4	688.5
5	-21.14	174.8	-479.9	930.5
6	-29.4	229.5	-716.5	1306

Table 9. Shear forces value statistics

Stages	Shear Q12		Shear Q13		Shear Q23	
	min	max	min	max	min	max
1		1.47E-07	-13.92	19.96		1.25E-07
2		5E-07	-62.69	53.48	5.13E-08	1.11E-06
3	-2.89E-07	7.82E-07	-112.6	89.9	6.50E-08	1.90E-06
4	-2.90E-07	8.73E-07	-173.6	108.6	7.09E-08	2.62E-06
5	-2.91E-07	8.46E-07	-265.8	112.8	7.10E-08	3.63E-06
6	-2.93E-07	7.88E-07	-414.3	167.6	7.08E-08	4.59E-06

The values presented indicate significant differences in the behavior of shear forces across three different shear directions, namely Q12, Q13, and Q23, across all stages (Table 9).

In the case of Shear Q12, the values remain relatively small and consistent, exhibiting minimal variations from 1.47E-07 to 8.73E-07 kN/m. This consistency suggests that the excavation process does not significantly affect shear forces in this direction, possibly due to the orientation of the excavation or the inherent structural properties resisting changes in this shear direction.

Conversely, Shear Q13 shows a substantial increase in both the maximum and minimum shear values as the excavation progresses, ranging from -13.92 kN/m to 19.96 kN/m in the first stage to -414.3 kN/m to 167.6 kN/m in the sixth stage. This trend indicates a growing imbalance or redistribution of forces within the structure as deeper layers are excavated, highlighting potential areas of structural stress or failure that could require reinforcement or careful monitoring.

Similarly, the maximum values for Shear Q23 escalate dramatically from 1.25E-07 kN/m in the initial stage to 4.59E-06 kN/m in the final stage. This progressive increase in shear forces could be indicative of increasing lateral pressures as the excavation depth increases, potentially compromising the stability of the excavation sides and necessitating the implementation of adequate shoring systems to prevent collapse.

Table 10. Torsion moments M12 value statistics

Stages	Torsion moments M12	
	min	max
1		1.98E-07
2	-1.8E-06	1.81E-06
3	-3.05E-06	3.04E-06
4	-4.18E-06	4.16E-06
5	-5.78E-06	5.76E-06
6	-7.30E-06	7.27E-06

The analysis of torsion moments M12 across the six stages of excavation reveals a consistent pattern of increase in both the maximum and minimum values (Table 10). Initially, the torsion moments are extremely low, with the first stage having a maximum value of only 1.98E-07 kN/m. This indicates minimal torsional stress at the commencement of excavation.

As excavation progresses to deeper levels, there is a significant increase in torsional moments, indicating increased structural stress. By the second stage, torsion moments fluctuate around zero, showing a slight increase to -0.000001812 kN/m and 0.000001808 kN/m for the minimum and maximum values, respectively. This shift from nearly negligible initial values suggests that the torsional demands on the structure begin to become more significant as the depth of excavation increases.

The trend continues with more pronounced increases through stages three to six. The third stage shows torsion moments at -3.05E-06 kN/m and 3.04E-06 kN/m, nearly doubling by the fourth stage to -4.18E-06 kN/m and 4.16E-06 kN/m. The increasing trend underscores the cumulative effect of excavation depth on torsional stresses within the structure.

By the fifth and sixth stages, torsion moments reach -5.78E-06 kN/m and 5.76E-06 kN/m, and -7.30E-06 kN/m and 7.27E-06 kN/m, respectively. These values illustrate a steady increase in torsional demands, reflecting the ongoing impact of successive excavation layers on structural integrity.

3.2. Statistical analysis of inspection

The results of ANOVA analysis given with the independent variable are the parameters Torsion moments, shear force, Bending moment, Axial forces, U, Ux, Uy, and Uz deformation values. The dependent variable is the stages.

The variables Ux, Uy, Uz, U, N1, N2, Q12, Q23, Q13, M11, M22, and M12 all have a P-value of 0.000, which indicates that there is a significant difference in variance between groups for each variable (Table 11). This implies that the assumption of homogeneity of variance is rejected at the level of statistical significance. Therefore, reviewing the Robust Test analysis results is necessary (Figure 2) in Table 12.

Table 11. Test of Homogeneity of Variances

	Levene Statistic	df1	df2	Sig.
Ux	388,483	5	2730	,000
Uy	550,886	5	2730	,000
Uz	246,247	5	2730	,000
U	741,690	5	2730	,000
N1	401,832	5	2730	,000
N2	139,325	5	2730	,000
Q12	130,977	5	2730	,000
Q23	320,255	5	2730	,000
Q13	123,458	5	2730	,000
M11	423,197	5	2730	,000
M22	195,237	5	2730	,000
M12	83,469	5	2730	,000

Table 12. Robust Tests of Equality of Means

		Statistic[a]	df1	df2	Sig.
Ux	Welch	264,606	5	1109,881	,000
Uy	Welch	1600,059	5	1115,924	,000
Uz	Welch	12643168,594	5	1197,841	,000
U	Welch	8531,537	5	1111,466	,000
N1	Welch	340,604	5	1098,680	,000
N2	Welch	269,004	5	1200,865	,000
Q12	Welch	364,783	5	1197,433	,000
Q23	Welch	550,395	5	1067,969	,000
Q13	Welch	10,313	5	1100,477	,000
M11	Welch	1233,368	5	1193,499	,000
M22	Welch	14,136	5	1068,621	,000
M12	Welch	,096	5	1069,925	,993

a. Asymptotically F distributed.

In the Robust Test table, the Sig values of the variables Ux, Uy, Uz, U, N1, N2, Q12, Q23, Q13, M11, and M22 are all 0, proving that these variables have differences between stages. Only variable M12 has Sig = 0.993, this variable has no difference between digging stages.

Use Games-Howell analysis to post-test to find the variable with the largest difference among the variables with differences between construction stages. The results of the Ux variable compared between stages have a significant difference (Sig. = 0.000), the Uy variable decreases significantly as the stages progress (from Stage 1 to Stage 2 the difference is -0.006072711, Sig. = 0.000), Uz is similar to Uy, Uz also decreases significantly in later stages (from Stage 1 to Stage 6, the difference is -0.018497660, Sig. = 0.000), U changes greatly across stages. Period (significant decrease from

Period 1 to Period 6, difference is -0.032850999, Sig. = 0.000), Group of variables N1 and N2 show a significant increase in later periods compared to previous periods (N1 increases from 121,921 at Stage 1 to Stage 2 up to 460,343 from Stage 1 to Stage 6 with Sig = 0.000), Groups Q12 and Q23 show a significant change, although the actual values are very different. small, reflecting small but statistically significant differences (Q12 from Phase 1 to Phase 2 is -0.000000187, Sig. = 0.000), M11 and M22 show significant changes across phases (M11 decreased from -27,638 in Stage 1 to Stage 2 to -134,048 from Stage 1 to Stage 6 with Sig. = 0.000).

In the analysis from the Games-Howell post hoc tests, the variable Uz exhibits the most substantial differences between stages. This difference is quantitatively significant and is represented with very precise statistical values. For instance, the mean difference between Stage 1 and Stage 3 for Uz is -0.011647417, with an exceptionally low standard error of 0.000002713 and a significance level (Sig.) of 0.000, indicating not only a significant difference but also one with high precision. The magnitude of the changes in Uz is notably larger than those observed in other variables, with p-values consistently indicating these differences are statistically significant.

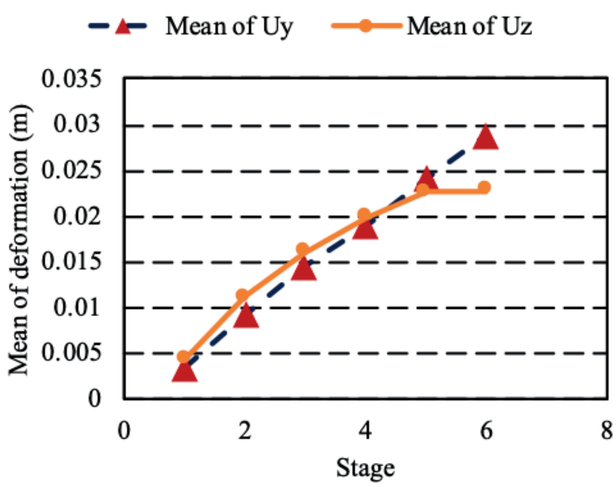

Figure 5. Mean plot of deformation Uy and Uz

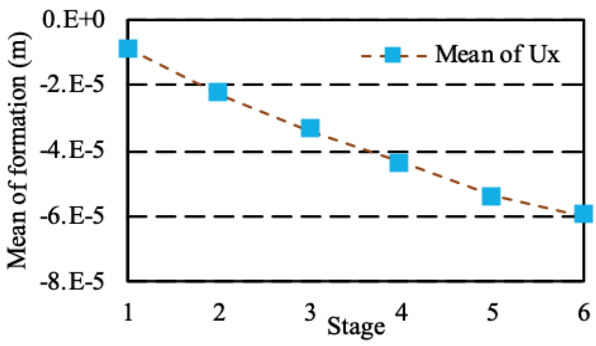

Figure 6. Mean plot of Ux

In addition to the variable Uz, which shows the most significant differences among the stages studied, attention should also be directed towards the variable Uy. This variable, similar to Uz, displays substantial stage-to-stage variations with consistently significant results, indicating its critical role in the study. Uy demonstrates a clear creasing trend as the stages progress, which could suggest a systematic change in the experimental conditions or the effect of accumulating variables across stages. The increment in Uy from Stage 1 to Stage 6 is notably significant, with the difference marked at 0.025413693, a p-value of 0.000 underscoring its importance in reflecting the underlying phenomena being studied (Figure 5).

Besides the variables that increase according to the stage, the variable Ux also decreases according to the construction stage (Figure 6).

3.3. Discussion

This research has underscored the critical importance of monitoring and evaluating deformations within geotechnical engineering projects, particularly those involving deep excavations like the one studied. The detailed analysis of deformation across different stages of the excavation process has highlighted significant transformations in the structure's behavior under varying geotechnical conditions. Integrating the Finite Element Method (FEM) with the Analysis of Variance (ANOVA), provides a nuanced understanding of the structural behaviors underpinning deep excavation projects, specifically focusing on barrette wall joints. The significance of the deformations observed at these joints, the underlying causes, and their implications for structural safety are crucial for refining construction practices and enhancing project outcomes. Through the FEM, we have been able to simulate detailed scenarios that reflect real-world conditions under which these deep excavations are subjected. The FEM results reveal that the deformation patterns are primarily influenced by the geometrical setup of the walls and the mechanical properties of the soils. For instance, the greatest deformations were typically observed where the wall joints experienced the highest bending moments and shear forces, conditions that are exacerbated by unfavorable soil mechanics and hydrostatic pressures. The ANOVA analysis further assists in decoding the influence of various factors such as load conditions, soil consistency, and construction stages on these deformations. Significant findings from the ANOVA suggest that variations in soil properties across different layers significantly affect the deformation outcomes. For example, softer soil layers were associated with higher degrees of deformation at wall joints. This relationship underscores the necessity for precise soil assessment and characterization in the planning stages of construction to mitigate potential risks.

In this context, the variable Uz, which records vertical displacements, has demonstrated the largest and most significant changes across all stages. These findings are particularly important as they provide clear evidence of the progressive destabilization that can occur as excavation depths increase. The substantial increases in deformation measurements from the earliest to the final stages suggest that the structural integrity of the excavation walls could be compromised without adequate monitoring and intervention. Additionally, the variable Uy, indicative of lateral displacements, also shows significant transformations, reinforcing the necessity of a comprehensive monitoring strategy that encompasses multiple axes of deformation. The clear decreasing trend in Uy values as the excavation progresses could indicate lateral shifts or bending of the walls under load, which, if not adequately braced, could lead to catastrophic failures. The interaction of these variables with the mechanical properties of the soil and the construction materials used (as detailed in the earlier tables of material properties and design specifics) provides a complex picture of the dynamic interactions within the excavation site. For instance, changes in soil moisture, which affect soil stiffness and permeability, could further exacerbate the deformation rates observed.

By comparing these results with existing studies, such as those by Arabaninezhad, A., & Fakher, A. (2021) who investigated similar deep excavation projects in urban environments, it becomes evident that our findings align with broader observations in the field. These studies also highlighted the critical impact of soil heterogeneity on wall stability and emphasized the value of integrated approaches in predicting and managing structural responses.

One of the critical insights from our study is the demonstration of how specific deformation patterns, identified statistically through ANOVA, correlate strongly with increased risks of structural failure. For instance, where significant statistical differences in deformation across stages of excavation were noted, these often coincided with stages where historical data indicate a higher incidence of structural failures. This correlation not only validates the FEM and ANOVA as effective tools for this field of study but also enhances our ability to predict and prevent failures.

Moreover, the application of these analytical methods allows for a proactive approach to construction management. By understanding which stages of the excavation process are most susceptible to critical deformations, project managers can implement targeted reinforcement strategies and adjust construction plans in real time to ensure structural integrity.

4. CONCLUSIONS

This research has provided comprehensive insights into the deformation behaviors of barrette wall joints under various construction conditions through the combined use of the Finite Element Method (FEM) and Analysis of Variance (ANOVA). By integrating these two powerful analytical tools, we have been able to pinpoint critical factors influencing structural deformations and thereby propose more effective risk management and mitigation strategies in geotechnical engineering projects. The application of FEM has allowed for a detailed simulation of the complex interplay between soil properties, wall geometry, and loading conditions. This method revealed that deformations at the barrette wall joints are significantly affected by variations in soil composition and moisture content, as well as by the physical constraints imposed by the surrounding structures. The results have highlighted the critical need for precise monitoring and evaluation mechanisms in geotechnical engineering projects, especially those involving significant changes in the structural environment. The variables Uz and Uy, which measure vertical and lateral displacements respectively, have shown significant increases in deformation with Uz experiencing a peak deformation of 0.0555 meters at the maximum excavation depth of -15 meters. This significant deformation underscores the progressive destabilization of the excavation walls as the depth increases. For instance, the increase in Uz from 0.0043 meters at the first stage to 0.023 meters in the final stage illustrates a more than fivefold increase in vertical displacement, which clearly indicates the gravity of structural shifts that could potentially lead to wall failures if not properly managed.

Similarly, Uy presented a significant reduction from an initial deformation at the first stage to a decrease by the sixth stage, which corresponds to the lateral adjustments of the wall under different loading conditions. These quantitative changes in Uy from 0.00455 meters in the initial stage to of 0.0480 meters by the final stage highlight the lateral movement tendencies that need continuous monitoring to prevent any unforeseen structural failures. Furthermore, the utilization of ANOVA has provided a robust statistical framework to assess the impact of these variables systematically, confirming the hypothesis that certain construction stages and soil conditions pose greater risks than others.

The major contributions of this study include the identification of specific stages in construction that are prone to critical deformations, and the clarification of how different soil layers' properties can drastically influence the stability of deep excavation sites. Such insights are invaluable for construction engineers and project managers, as they highlight the need for tailored construction strategies based on the specific conditions of each site. Additionally, the research findings advocate for the implementation of continuous monitoring systems at construction sites to dynamically assess and respond to potential structural failures. Real-time data obtained from such systems can be analyzed using the methodologies described in this study to make immediate adjustments to the construction process, thereby enhancing safety and efficiency. For future research, it is recommended to expand the application of these methodologies to a wider range of geotechnical structures and conditions. Investigating different types of soil and more varied construction scenarios will further validate the versatility and robustness of the FEM and ANOVA integration. Moreover, longitudinal studies that track structural integrity over time post-construction could provide deeper insights into the long-term impacts of the identified factors on structural health and safety.

In practical terms, this study serves as a foundation for developing advanced predictive models that can be incorporated into construction planning and management software. These models, equipped with the ability to simulate various scenarios and predict outcomes, could significantly improve decision-making processes in construction projects, especially those involving complex underground constructions. By identifying key factors affecting structural integrity and demonstrating the effective use of advanced analytical techniques, this study contributes to the enhancement of safety standards and the optimization of construction practices globally.

REFERENCES

1. **Nguyen, N.-N., L.H. To, and B.V. Le**. Behavior of Isotropic and Anisotropic Diaphragm Walls in Finite Element Analysis Model of Deep Excavation. in The International Conference on Sustainable Civil Engineering and Architecture. 2023. Springer.
2. **Qiao, Y.-K., et al.**, Socio-environmental costs of underground space use for urban sustainability. Sustainable Cities and Society, 2019. 51: p. 101757.
3. **Council, N.R., et al.,** Underground engineering for sustainable urban development. 2013: National Academies Press.
4. **Espinosa, H.D., et al.,** Merger of structure and material in nacre and bone–Perspectives on de novo biomimetic materials. Progress in Materials Science, 2009. 54(8): p. 1059-1100.
5. **Bardenhagen, S., A. Brydon, and J. Guilkey,** Insight into the physics of foam densification via numerical simulation. Journal of the Mechanics and Physics of Solids, 2005. 53(3): p. 597-617.
6. **Gelman, A.,** Analysis of variance—why it is more important than ever. 2005.
7. **Christensen, R.,** Analysis of variance, design, and regression: applied statistical methods. 1996: CRC press.
8. **Alzyod, H. and P. Ficzere,** Material-dependent effect of common printing parameters on residual stress and warpage deformation in 3D printing: A comprehensive finite element analysis study. Polymers, 2023. 15(13): p. 2893.
9. **Li, C., et al.,** Aero-mechanical multidisciplinary optimization of a high speed centrifugal impeller. Aerospace Science and Technology, 2019. 95: p. 105452.
10. **Sivareddy, D.V., et al.,** Parameter optimisation in vibration assisted turning of Ti6Al4V alloy using ANOVA and grey relational analysis. International Journal of Automotive and Mechanical Engineering, 2018. 15(3): p. 5400-5420.
11. **Read, R.,** 20 years of excavation response studies at AECL's Underground Research Laboratory. International Journal of Rock Mechanics and Mining Sciences, 2004. 41(8): p. 1251-1275.
12. **Martino, J. and N. Chandler,** Excavation-induced damage studies at the underground research laboratory. International Journal of Rock Mechanics and Mining Sciences, 2004. 41(8): p. 1413-1426.
13. **Do, T., et al.,** A combined finite difference and finite element model for temperature and stress predictions of cast-in-place cap beam on precast columns. Construction and Building Materials, 2019. 217: p. 172-184.
14. **Cashman, P.M. and M. Preene,** Groundwater lowering in construction: a practical guide to dewatering. 2020: CRC Press.
15. **Council, N.R., et al.,** Alternatives for managing the nation's complex contaminated groundwater sites. 2013: National Academies Press.
16. **Powers, J.P., et al.,** Construction dewatering and groundwater control: new methods and applications. 2007: John Wiley & Sons.
17. **David, T.K., R.R. Krishnamoorthy, and M.J. IB,** Finite element modelling of soil-structure interaction. Jurnal Teknologi, 2015. 76(8).
18. **Phuor, T., et al.,** Development of the skew boundary condition for soil-structure interaction in three-dimensional finite element analysis. Computers and Geotechnics, 2021. 137: p. 104264.
19. **IBST,** Geological survey report file. 2016.
20. **Hox, J. and H. Hoijtink,** Analysis of Variance: Why It Is More Important than Ever: Discussion. The Annals of Statistics, 2005. 33(1): p. 39-42.
21. **Levine, D.W., et al.,** A self-administered questionnaire for the assessment of severity of symptoms and functional status

in carpal tunnel syndrome. JBJS, 1993. 75(11): p. 1585-1592.
22. **Kim, Y.-K., S.-M. Kim, and H. Myoung,** Musical intervention reduces patients' anxiety in surgical extraction of an impacted mandibular third molar. Journal of oral and maxillofacial surgery, 2011. 69(4): p. 1036-1045.
23. **Leandri, M., et al.,** Balance features in Alzheimer's disease and amnestic mild cognitive impairment. Journal of Alzheimer's Disease, 2009. 16(1): p. 113-120.
24. **O'Toole, S., et al.,** Investigation into the accuracy and measurement methods of sequential 3D dental scan alignment. Dental Materials, 2019. 35(3): p. 495-500.
25. **Trattnig, S., et al.,** Lumbar intervertebral disc abnormalities: comparison of quantitative T2 mapping with conventional MR at 3.0 T. European radiology, 2010. 20: p. 2715-2722.
26. **Wang, J., et al.,** Multi-source data integration and multi-scale modeling framework for progressive prediction of complex geological interfaces in tunneling. Underground Space, 2024. 15: p. 1-25.

СПИСОК ЛИТЕРАТУРЫ

1. **Nguyen, N.-N., L.H. To, and B.V. Le**. Behavior of Isotropic and Anisotropic Diaphragm Walls in Finite Element Analysis Model of Deep Excavation. in The International Conference on Sustainable Civil Engineering and Architecture. 2023. Springer.
2. **Qiao, Y.-K., et al.**, Socio-environmental costs of underground space use for urban sustainability. Sustainable Cities and Society, 2019. 51: p. 101757.
3. **Council, N.R., et al.,** Underground engineering for sustainable urban development. 2013: National Academies Press.
4. **Espinosa, H.D., et al.,** Merger of structure and material in nacre and bone–Perspectives on de novo biomimetic materials. Progress in Materials Science, 2009. 54(8): p. 1059-1100.
5. **Bardenhagen, S., A. Brydon, and J. Guilkey,** Insight into the physics of foam densification via numerical simulation. Journal of the Mechanics and Physics of Solids, 2005. 53(3): p. 597-617.
6. **Gelman, A.,** Analysis of variance—why it is more important than ever. 2005.
7. **Christensen, R.,** Analysis of variance, design, and regression: applied statistical methods. 1996: CRC press.
8. **Alzyod, H. and P. Ficzere,** Material-dependent effect of common printing parameters on residual stress and warpage deformation in 3D printing: A comprehensive finite element analysis study. Polymers, 2023. 15(13): p. 2893.
9. **Li, C., et al.,** Aero-mechanical multidisciplinary optimization of a high speed centrifugal impeller. Aerospace Science and Technology, 2019. 95: p. 105452.
10. **Sivareddy, D.V., et al.,** Parameter optimisation in vibration assisted turning of Ti6Al4V alloy using ANOVA and grey relational analysis. International Journal of Automotive and Mechanical Engineering, 2018. 15(3): p. 5400-5420.
11. **Read, R.,** 20 years of excavation response studies at AECL's Underground Research Laboratory. International Journal of Rock Mechanics and Mining Sciences, 2004. 41(8): p. 1251-1275.
12. **Martino, J. and N. Chandler,** Excavation-induced damage studies at the underground research laboratory. International Journal of Rock Mechanics and Mining Sciences, 2004. 41(8): p. 1413-1426.
13. **Do, T., et al.,** A combined finite difference and finite element model for temperature and stress predictions of cast-in-place cap beam on precast columns. Construction and Building Materials, 2019. 217: p. 172-184.

14. **Cashman, P.M. and M. Preene,** Groundwater lowering in construction: a practical guide to dewatering. 2020: CRC Press.
15. **Council, N.R., et al.,** Alternatives for managing the nation's complex contaminated groundwater sites. 2013: National Academies Press.
16. **Powers, J.P., et al.,** Construction dewatering and groundwater control: new methods and applications. 2007: John Wiley & Sons.
17. **David, T.K., R.R. Krishnamoorthy, and M.J. IB,** Finite element modelling of soil-structure interaction. Jurnal Teknologi, 2015. 76(8).
18. **Phuor, T., et al.,** Development of the skew boundary condition for soil-structure interaction in three-dimensional finite element analysis. Computers and Geotechnics, 2021. 137: p. 104264.
19. **IBST,** Geological survey report file. 2016.
20. **Hox, J. and H. Hoijtink,** Analysis of Variance: Why It Is More Important than Ever: Discussion. The Annals of Statistics, 2005. 33(1): p. 39-42.
21. **Levine, D.W., et al.,** A self-administered questionnaire for the assessment of severity of symptoms and functional status in carpal tunnel syndrome. JBJS, 1993. 75(11): p. 1585-1592.
22. **Kim, Y.-K., S.-M. Kim, and H. Myoung,** Musical intervention reduces patients' anxiety in surgical extraction of an impacted mandibular third molar. Journal of oral and maxillofacial surgery, 2011. 69(4): p. 1036-1045.
23. **Leandri, M., et al.,** Balance features in Alzheimer's disease and amnestic mild cognitive impairment. Journal of Alzheimer's Disease, 2009. 16(1): p. 113-120.
24. **O'Toole, S., et al.,** Investigation into the accuracy and measurement methods of sequential 3D dental scan alignment. Dental Materials, 2019. 35(3): p. 495-500.
25. **Trattnig, S., et al.,** Lumbar intervertebral disc abnormalities: comparison of quantitative T2 mapping with conventional MR at 3.0 T. European radiology, 2010. 20: p. 2715-2722.
26. **Wang, J., et al.,** Multi-source data integration and multi-scale modeling framework for progressive prediction of complex geological interfaces in tunneling. Underground Space, 2024. 15: p. 1-25.

Phuong Tuan Nguyen, Doctor of Phylosophy, Lecturer, Mien Tay Construction University, Vinh Long Province, VIETNAM, 20B Pho Co Dieu, Ward 3, Vinh Long City. Mobile: +84919070096. Email: tuanphuongvk@gmail.com

Фыонг Туан Нгуен, к.т.н., преподаватель, Миентай строительный университет, Виньлонг, ВЬЕТНАМ, 20B ул. Co Dieu, город Виньлонг. Мобильный: +84919070096. Электронная почта: tuanphuongvk@gmail.com

Truong Xuan Dang, Doctor of Phylosophy, Lecturer, Ho Chi Minh University of Natural Resources and Environment, Ho Chi Minh City, VIETNAM, No 236B Le Van Sy, Tan Binh district. Mobile: +84913804068. Email: dxtruong@hcmunre.edu.vn

Чыонг Суан Данг, к.т.н., преподаватель, Хошиминский университет природных ресурсов и окружающей среды, Хошимин, ВЬЕТНАМ, № 236B Ле Ван Си, район Тан Бинь. Мобильный: +84913804068. Электронная почта: dxtruong@hcmunre.edu.vn

Thuan Anh Nguyen, Associate Professor, Lecturer, Department of Railways and Metro, University of Transport Ho Chi Minh City, Ho Chi Minh City, 717066, VIETNAM, No 2, Vo Oanh street, Binh Thanh district. Mobile: +849839097793. Email: tuanna@ut.edu.vn

Туан Ань Нгуен, к.т.н., доцент, преподаватель кафедры железных дорог и метро, Хошиминский университет транспорта, г. Хошимин, 717066, ВЬЕТНАМ, № 2, улица Во Оан, район Бинь Тхань. Мобильный: +849839097793. Электронная почта: tuanna@ut.edu.vn

Hoa Van Vu Tran, Expert of the SDCT Research Group, University of Transport Ho Chi Minh City, Ho Chi Minh City, 717066, VIETNAM, No 2, Vo Oanh street, Binh Thanh district. Mobile: +84902227137. Email: hoa.tranvu.htgroup@gmail.com

Хоа Ван Ву Чан, эксперт исследовательской группы SDCT, Хошиминский университет транспорта, Хошимин, 717066, ВЬЕТНАМ, № 2, улица Во Оан, район Бинь Тхань. Мобильный: +84902227137. Электронная почта: hoa.tranvu.htgroup@gmail.com